ISSN 0010-9525, Cosmic Research, 2024, Vol. 62, No. 2, pp. 133–146. © Pleiades Publishing, Ltd., 2024.

# Sources of Solar Protons in the Events of February 24–25 and July 16–17, 2023

**A. B. Struminsky[a], *, A. M. Sadovskii[a], and I. Yu. Grigorieva[b]**

[a] *Space Research Institute of the Russian Academy of Sciences, Moscow, 117997 Russia*

[b] *Main (Pulkovo) Astronomical Observatory of the Russian Academy of Sciences, St. Petersburg, 196440 Russia*

**e-mail: astruminsky@gmail.com*

Received September 1, 2023; revised October 15, 2023; accepted October 17, 2023

**Abstract**—From the beginning of January 2021 to the end of August 2023, the radiation monitor of the *Spektr-RG* spacecraft registered three enhancements in the count rate, which exceed the background variations during the solar activity cycle and have a comparable maximum value. These enhancements are associated with solar proton events (SPEs) from the flares X1.0 on October 28, 2021; M6.3 on February 25, 2023; and M5.7 on July 17, 2023. Using the example of these events, as well as smaller SPEs from the flares M3.7 on February 24, 2023, and M4.0 on July 16, 2023, threshold criteria for "proton" flares are discussed. In powerful SPEs, the contribution of solar protons to the radiation dose can exceed the total contribution of galactic cosmic rays (GCR) over a sufficiently long period of time. Therefore, such SPEs are sources of increased radiation hazard and require prediction based on real-time observations. It was shown that, in these five flares, thresholds were overcome according to three criteria: plasma temperature >12 MK (soft X-ray source), duration (>5 min) of microwave or hard X-ray (HXR) radiation (electron acceleration >100 keV), and height of flare development process >60 Mm (radio emission at plasma frequencies <610 MHz). The arrival of the first solar protons >100 MeV to the Earth's orbit was expected no earlier than 10 min relative to the beginning of HXR or microwave radiation, i.e., could have been predicted in advance. To study the relationship between solar flares and SPEs, we used data from the anticoincidence shield of the spectrometer on *INTEGRAL* (ACS SPI), which is an effective but uncalibrated detector of HXR >100 keV and protons >100 MeV, as well as patrol observations of radio emission at fixed frequencies (Radio Solar Telescope Network). It is noted that the X2.2 (N25E64) flare on February 17, 2023 satisfied all three "protonity" criteria and could become the source of a powerful SPE near the Earth in a case of favorable location on the Sun. In the M8.6 (N27W29) flare on February 28, 2023, the third criterion was not met, and it did not lead to an SPE as expected (it developed in a plasma with a density $>2.5 \times 10^{10}$ cm$^{-3}$ and plasma frequency >1415 MHz).

**DOI:** 10.1134/S0010952523600300

## INTRODUCTION

The Mikhail Pavlinsky *SRG/ART-XC* telescope has sensitive detectors for registering primary X-ray radiation from weak distant sources, and so secondary X-ray radiation from cosmic rays (CR) is a harmful background for it ($E_{HXR} > 60$ keV). During the solar proton event (SPE) on October 28, 2021 [1–3], accompanied by a ground-level enhancement in CR intensity (GLE), detectors ART-XC recorded a fourfold increase in the background. Management of the *ART-XC* decided to make information about the radiation situation at the Lagrange point *L*2 publicly available and start posting data about the detector background on the website (https://monitor.srg.cosmos.ru). The radiation monitor *SRG/ART-XC* provides the average count rate of detectors over 10 min (light curves) in the energy range of 60–120 keV with a delay of 1 day. The user can plot counting tempo curves *ART-XC* for various periods of time from the last 3 days to the entire observation time.

Figure 1a shows a screenshot of the screen at the moment when the light curve of the radiation monitor was plotted from the beginning of January 2021 to the end of August 2023. At this time scale, the effect of CR modulation in the solar activity cycle is clearly visible (October 2021 is the growth phase near the minimum of the 24th–25th cycle, and July 2023 is the growth phase near the cycle maximum). The modulation depth depends on the GCR energy and varies from a few percent at equatorial neutron monitors (NMs) to ~20% at polar NMs, up to hundreds of percent for measurements in the stratosphere, and up to an order of magnitude in outer space [4]. Figure 1a shows three increases that exceed the GCR background variations in the activity cycle, have comparable intensity and are associated with the arrival of solar cosmic rays (SCR). The contribution of one powerful SPE to the radiation dose can exceed the total contribution from the GCR

over a long period of time. It is precisely such events that need to be forecast from real-time observations to ensure safe space activities. The smaller events are of only limited, mostly academic interest.

According to the catalog of proton events of the 25th cycle (https://swx.sinp.msu.ru/apps/sep_events_cat/index.php?gcm=1&lang=ru) with these three large increases in the counting rate of the radiation monitor of the *SRG/ART-XC* (Fig. 1a), five SPEs can be associated—October 28, 2021; February 24 and 25, 2023; and July 16 and 18, 2023. On a time scale of the order of several days, it is clear that the monitor of the *SRG/ART-XC* (Fig. 1b) did not register an increase from the SPE on February 24, 2023, and in the SPE on July 16, 2023 (Fig. 1c) there were two successive increases, possibly from different solar sources.

The event of October 28, 2021, fully fits the concept of acceleration of solar protons >100 MeV [5] in long-term eruptive flares against the background of acceleration of coronal mass ejections (CMEs). The period of time in flares in which protons are accelerated lasts several minutes or more and is characterized by plasma temperature >12 MK, emitting soft X-rays (SXR) rays; acceleration of electrons to energies >100 keV (i.e., by hard X-rays (HXR) >100 keV and/or microwave radiation at frequencies >1.5 GHz); and the development of the flare process upward into the corona (plasma radiation at frequencies <610 MHz) [6]. The result of the development of the flare process upward into the corona is acceleration of the CME. The absence of radio emission at frequencies <1415 MHz is typical for flares without CME and SPE of the 23rd and 24th solar cycles studied in [7] and [8, 9], respectively.

In article [6], it was suggested that the acceleration of protons with energies above 1 MeV is possible at an electron plasma temperature of ~10 MK. At this temperature, the velocities of thermal electrons and ~1-MeV protons are approximately equal, which can help maintain electrical neutrality of the plasma while accelerating protons and electrons. It also follows from the principle of electrical neutrality that, during the interaction of protons in a plasma, the generation of $\pi_0$-mesons will be possible at an electron energy of ~150 keV (protons with $E \sim 300$ MeV are equivalent in speed to electrons with $E \sim 150$ keV). Consequently, the acceleration of solar protons >100 MeV should occur against the background of microwave (GHz) or HXR radiation with $E > 100$ keV.

For protons to reach velocities equal to the velocities of electrons, it takes a time at least $m_p/m_e$ times greater. Therefore, the key point for estimating the acceleration time of protons is the time of acceleration of electrons to energies of ~100 keV [10], which determines the required duration of observation of HXR radiation with $E > 100$ keV and/or microwave radiation, as well as the expected moment of arrival of the first accelerated protons to Earth during free propagation in interplanetary space (IS).

Observational data show that the acceleration time of electrons to a kinetic energy of ~100 keV is on the order of ~400 ms [11]. Delays between HXR bursts at different electron energies (20, 50, 100, 200, and 300 keV) of the order of tens of milliseconds are also observed, which may be due to the electron acceleration time [12, 13]. Therefore, the time required for proton recruitment $E \sim$ 200 MeV will be ~1 min when electrons are accelerated to a kinetic energy of ~100 keV in 40 ms ("fast" acceleration) or ~10 min when electrons are accelerated to ~100 keV in 400 ms ("slow" acceleration) [6].

If we take the beginning of microwave radiation at 8.8–15.4 GHz to be zero time in solar events (it usually coincides with the appearance of a significant HXR emission signal with $E \sim 100$ keV), then the expected time of arrival of protons with $E \sim 200$ MeV ($V/c = 0.57$) into the Earth's orbit will be ~11 and ~21 min with "fast" and "slow" acceleration, respectively, and subsequent propagation without scattering along the Parker spiral to the Earth (1.3 AU, solar wind speed 300 km/s). Thus, the indeterminability of the characteristic time of acceleration of solar electrons to $E \sim$ 100 keV causes indeterminability of the time of the first arrival of solar protons from $E \sim 200$ MeV per Earth orbit and is about 10 min [6]. The required time (characteristic size) for the acceleration of protons >100 MeV is most likely determined by the upward development of the flare process associated with the acceleration of the CME. Also, the indeterminability of about 11 min fits into the effect of velocity dispersion between protons of 100 MeV ($V/c = 0.43$) and 500 MeV ($V/c = 0.76$).

These ideas were developed by us in [6] and became the basis for proposals for ultra-urgent SPE forecasting in real time [14]. During a solar flare accompanied by an SPE, four energy thresholds must be sequentially overcome: regarding the temperature of the flare plasma, regarding the energy and duration of electron acceleration, regarding the development of the process upward into the corona, and regarding the acceleration of an interplanetary CME (>618 km/s on the solar surface).

The goal of the work is to answer the question of whether these five SPEs can be predicted in advance from observed solar electromagnetic radiation (EMR) in real time. The work links the SPEs observed at this time to specific solar flares; the necessary rate of acceleration of protons on the Sun was determined to explain the observed time of the first arrival of solar protons into the Earth's orbit; criteria for predicting "proton" flares were discussed [14]. For comparison, these five events are supplemented by two more solar flares, on February 17 and 28, 2023, from which no solar energetic protons were detected.

## INSTRUMENTS AND METHODS

The currently available time resolution of the radiation monitor of the *ART-XC* does not allow solving

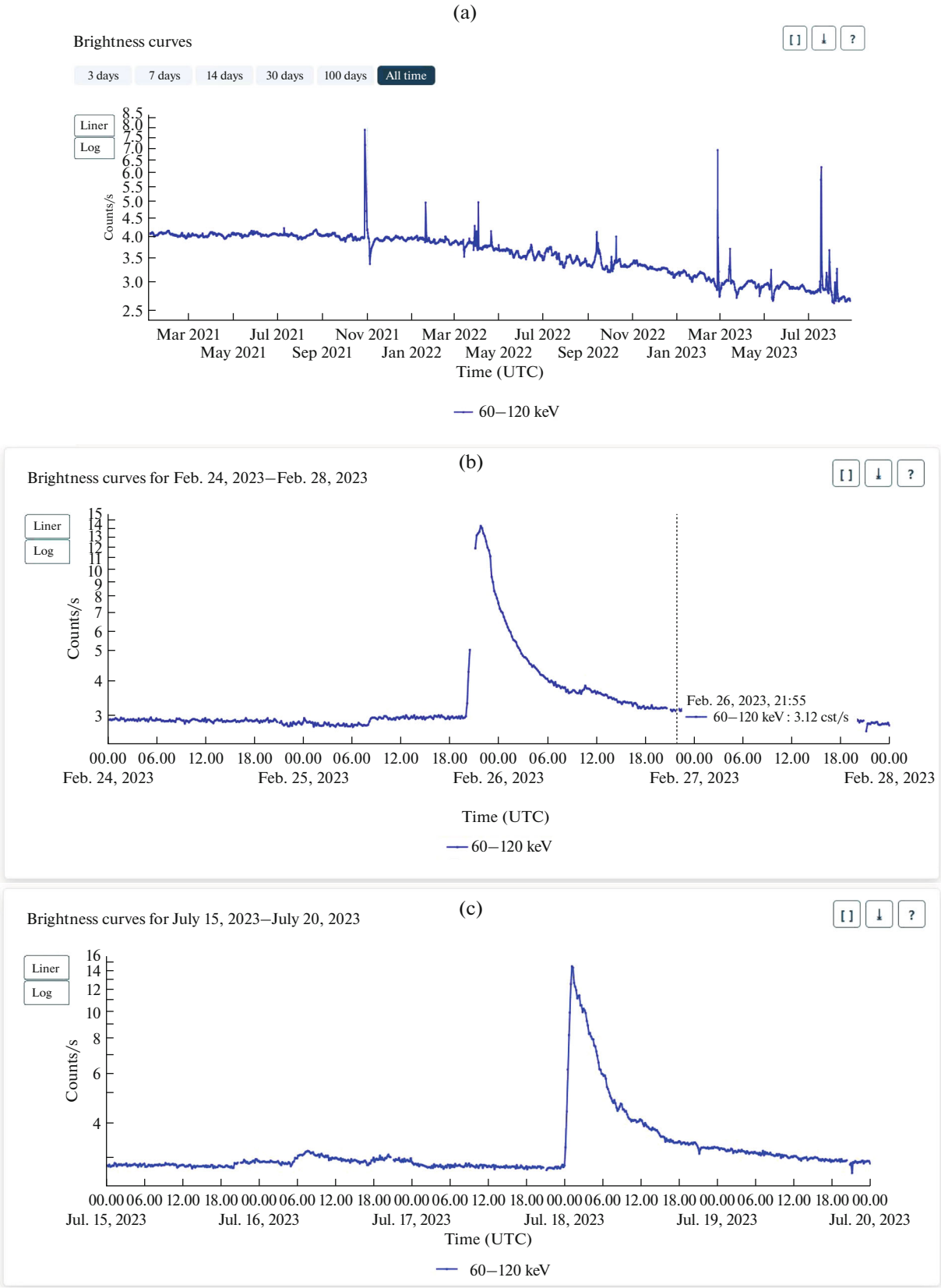


**Fig. 1.** Radiation situation at point *L*2 according to *JWG*/ART-XC data. (a) From the beginning of January 2021 to the end of August 2023; (b) from February 24 to 28, 2023; (c) from July 15 to 20, 2023.

the assigned problems, in particular, there is no way to separate primary solar HXR and secondary HXR (associated with the arrival of solar protons). The work investigated the proton increases of the monitor of the *ART-XC* using data from other detectors; i.e., the inverse problem of their forecast was solved—the sequence of characteristics of the parent solar flare that led to the SPE were determined. If such a sequence of characteristics is observed in the future, then, after 10–20 min, we should expect the beginning of a proton increase of >100 MeV.

The anticoincidence shield of the spectrometer on *INTEGRAL* (ACS SPI) registers HXR with $E > 100$ keV. These can be both primary photons and secondary photons generated in the detector body under the influence of protons with $E > 100$ MeV. The ACS SPI protection is an effective but uncalibrated HXR and proton detector. Using its data, we have previously studied the relationship between solar flares and proton events (for example, see [5, 6, 9, 10]). ACS SPI data are available at https://isdc.unige.ch/ ~savchenk/spiacs-online/spiacspnlc.pl with a time resolution of 50 ms. With 1-min smoothing and background subtraction, the ACS SPI counting rate becomes significant—less than ten counts per 50 ms [9]. The increase in the ACS SPI count rate during solar radio emission observations is caused by solar HXR emission. We consider the moment of the first arrival of solar protons into the Earth's orbit to be the beginning of a significant increase in the counting rate against the background or after a burst of solar HXR radiation [6].

To monitor the intensity of fluxes of protons with energies <100 MeV and relativistic electrons in interplanetary space near the Earth, data from proton channels (7.8–25 and 25–53 MeV) and electron channels of the electron–proton helium instrument (EPHIN) detector [15] onboard the spacecraft *SOHO*, which is located at Lagrange point *L*1. *SOHO* EPHIN data were taken from the website www2.physik.uni-kiel.de/SOHO/phpeph/EPHIN.htm. SPE analysis uses estimates of the maximum proton flux with $E > 10$ MeV, indicated in the SPE catalog of the 25th solar activity cycle of the Skobeltsyn Institute for Nuclear Physics of Moscow State University (https://swx.sinp.msu.ru/apps/sep_events_cat/index.php?gcm=1&lang=ru).

Temperature $T$ and emission measure $EM$ of flare plasma were calculated from 2-s integral fluxes of SXR radiation in channels 1–8 and 0.5–4 Å of the detector of the *GOES* spacecraft detector (/satdat.ngdc.noaa.gov/sem/goes/data/) in the SolarSoft package in the single-temperature approximation.

This work uses information about radio emissions presented in the YYYYMMDDevents.txt files (https://cdaw.gsfc.nasa.gov/CME_list/NOAA/org_events_text/2023/). These files contain information about the beginning, maximum, and end of observed radio emissions on the eight Radio Solar Telescope Network (RSTN) patrol frequencies. At four of them (15.4, 8.8, 4.995, and 2.695 GHz), predominantly gyrosynchrotron radiation is recorded, and plasma radiation is recorded at three (610, 410, and 245 MHz); at a frequency of 1415 MHz, the contribution of both mechanisms is possible. Primary electron acceleration in CME flares occurs at locations with a plasma frequency of ~500 MHz [16]. On the basis of measure $EM$ and observed plasma frequencies $v_p = 9000\sqrt{n}$, it is possible to make estimates of the size of the SXR source $R = \left(EM2n^2\right)^{13}$ [17].

The development of the flare process upward into the corona is evidenced by radio bursts at frequencies <180 MHz: type II is a slowly drifting burst, usually associated with the propagation of a shock wave in the corona; type IV with a wide, smooth and continuous spectrum, which is associated with acceleration and capture of electrons in the posteruptive arcade; type V is a short continuous burst, usually associated with a series of type III bursts–fast drifting bursts; and CTM is a broadband, long-lived, continuous decameter burst. Article [18] developed a method for predicting SPE based on observations of only type II and IV bursts. Theoretical approaches to type V radio bursts were developed in [19].

Table 1 presents the main characteristics of the considered SPEs and solar flares. Data on CME observations are taken from the electronic catalog SOHO LASCO CME CATALOG (/cdaw.gsfc.nasa.gov/CME_list/) [20]. All events are numbered in chronological order. Events are examined relative to the selected zero time. The beginning of the increase in HXR emission intensity was chosen as zero time if it was observed by the ACS SPI. Otherwise, the beginning of the growth of microwave radiation at the highest frequency observed by the RSTN is taken as the zero time.

## ACS SPI COUNT RATE FOR THE EVENTS OF FEBRUARY 24–25 AND JULY 16–18, 2023

The increases in the ACS SPI proton signal in events 1, 3, 4, and 7 are clearly associated with solar flares (Table 1), but there is no certainty in event 6. In the catalog of the 25th cycle (https://swx.sinp.msu.ru/apps/sep_events_cat/index.php?gcm=1&lang=ru), the SPE on July 16, 2023, with its onset at 05.40 UT and maximum at 07.35 UT, is associated with the C3.7 flare on July 15 at 21.04 UT with coordinates N24E25. We clearly see two proton increases in ACS SPI starting at ~04.57 UT (6a) and ~17.51 UT (6b). The nature of the ACS SPI light curves allows us to associate the increase in event 6a with coronal radio emission and the C1.9 flare, and the increase in event 6b with the M4.0 flare (Table 1). In event 6b, the observed GCR and SCR proton fluxes could have been modulated by the interplanetary structure after 18.00 UT (22 min).

**Table 1.** General characteristics of flashes and CMEs

| Options | Events | | | | | | | |
|---|---|---|---|---|---|---|---|---|
| | 1 | 2 | 3 | 4 | 5 | 6a | 6b | 7 |
| A | October 28, 2021 15.27 UT | February 17, 2023 19.57 UT | February 24, 2023 20.23 UT | February 25, 2023 19.23 UT | February 28, 2023 17.43 UT | July 16, 2023 04.33 UT | July 16, 2023 17.38 UT | July 17, 2023 23.25 UT |
| B | S26W05 2N 2887 | N25E64 2B 3229 | N28W28 2B 3229 | N26W43 3N 3229 | N27W29 3234 | S23W49 SF 3363 | S23W58 2B 3363 | S26W87 3363 |
| C | X1.0 −10 | X2.2 −19 | M3.7 −20 | M6.3 −43 | M8.6 −8 | C1.9 +16 | M4.0 −2 | M5.7 −7 |
| D | *0 +17* | *−5 >+100* | *−3 +10* | *−6 +40* | *−3 +14* | *?* | *+2 +15* | *−3 +25* |
| E | *0 +20* | *0 No* | *No +25* | *0 +25* | *No No* | *No +30* | *0 +13* | *0 +30* |
| F | *15400 0 +10* | *15400 0 +19* | *15400 0 +1* | *8800 +5 +17* | *15400 0 +5* | *245 0 +5* | *15400 0 +3* | *15400 +10 +21* |
| G | *245 0 +25* | *245 −8 −7* | *245 −4 +3* | *410 +3 +22* | *2695 −1 0* | *245 0 +5* | *245 −1 +6* | *245 −12 +25* |
| H | *IV +5 +102* | *No* | *IV +5 +216* | *CTM −130 +276* | *No* | *CTM 1 +291* | *V 0 +14* | *CTM 35 +374* |
| I | *+2 +26* | *0 +39* | *No* | *0 +14* | *No* | *No* | *No* | *No* |
| J | *+21 1526 189* | *+15 1315 56* | *+13 1336 345* | *+1 1170 294* | *No* | *+9 1970 275* | *+15 1239 220* | *+11 1385 223* |
| K | 22 | Background | 0.75 | 35 | Background | 18 | ? | 614 |

A is the date of the event and zero time; B is the coordinates, optical score, active region number; C is the score and beginning of the SXR flare; D is the beginning and end of SXR temperature according to *GOES* data (>12 MK); E is the beginning of registration of ACS SPI solar HXR radiation and beginning of proton increase of ACS SPI; F is the highest recorded RSTN frequency in MHz and the beginning and end of the increase; G is the lowest recorded RSTN frequency in MHz and the beginning and end of the increase; H is the type of continuous radio emission, <180 MHz, beginning and end; I is the beginning and end of type II radio emission; J is the time (UT) of the first appearance of the CME in the LASCO field of view and the average speed km/s, angle PA; K is units of proton flux >10 MeV in Earth orbit (1 pfu = 1 $(cm^2\ s\ sr)^{-1}$). In rows C to J, time is given in minutes relative to zero in each event.

Note that this binding of the proton increase (6a) contradicts the criteria [14] for predicting an SPE—the plasma temperature did not rise above 12 MK, there was no recorded HXR or microwave radiation, which does not exclude an source of protons behind the limb. Indeed, the spectrometer/telescope for imaging X-rays (STIX) X-ray telescope onboard the *Solar Orbiter* spacecraft, which was located in the heliosphere on the opposite side of the Sun from the Earth, registered an HXR burst on July 16, 2023, at 04.33 UT (https://datacenter.stix.i4ds.net/view/ql/lightcurves). According to the STIX catalog, the burst is associated with the C1.9 flare recorded by *GOES* near the Earth. The burst amplitude, converted to SXR *GOES* range, corresponds to a score of X9 (with a possible error from X4 to X19).

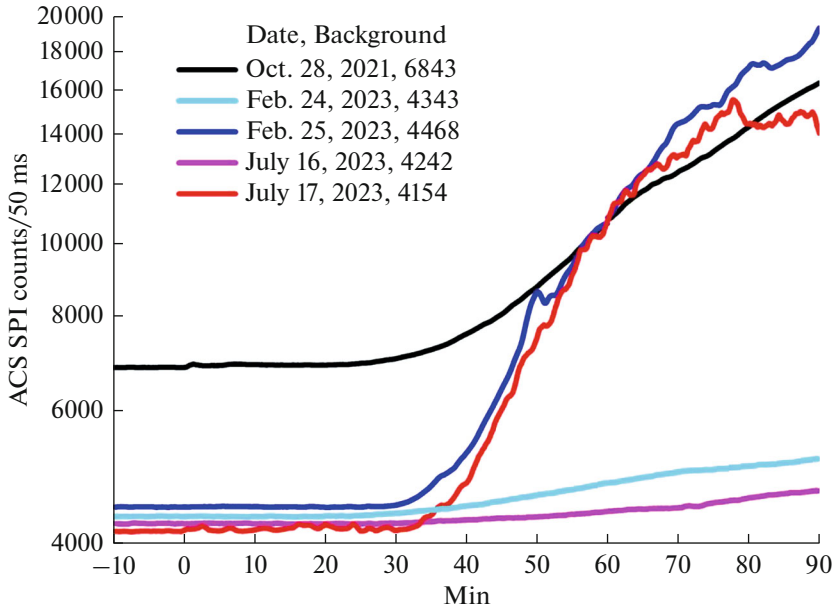


**Fig. 2.** Full 50-ms ACS SPI count rate, smoothed over 1 min, near event time zero:event 1—October 28, 2021; event 3—February 24, 2023; event 4—February 25, 2023; event 6a—July 16, 2023; and event 7—July 17, 2023 (see Table 1).

Figure 2 shows the 1-min smoothed ACS SPI count rate over 50 ms in events 1, 3, 4, 6a, and 7. The GCR modulation depth between October 28, 2021 and July 17, 2023 is 39.3%. This shows that ACS SPI is sensitive to protons of lower energy than polar NMs (atmospheric cutoff energy ~450 MeV). Proton intensity GCR > 100 MeV at maximum $J_{GCR} \sim 0.1$ (cm$^2$ s sr)$^{-1}$ matches background counting tempo $N_{background1}$ = 6843 pulses/50 ms (October 28, 2021), in an SPE with an amplitude greater than the GCR modulation, the proton flux > 100 MeV should be $J_{100} \sim 0.393 \times 0.1 > 0.04$ (cm$^2$ s sr)$^{-1}$.

$J_{100}$ in the SPE can be assessed according to ACS SPI if one knows background score $N_{background}$ and observed count $N$: $J_{100} = J_{GCR}\left(N - N_{background}\right)/N_{background\ 1}$. The results of these estimates are given in Table 2. The observed maximum proton flux >10 MeV in event 1 was $J_{10} = 22$ (cm$^2$ s sr)$^{-1}$, and in event 7 $J_{10}$ = 614 (cm$^2$ s sr)$^{-1}$ (see Table 1). For power spectrum $J = AE^{-\gamma}$, the assessment of its indicator will be $\gamma = \left(\log J_{10} - \log J_{100}\right)/\left(\log E_{100} - \log E_{10}\right)$. Substituting the numbers for events 1 and 7, we obtain, respectively, $\gamma = 1.7$ and 3.4. If, to determine $J_{10}$, we take $J_{100}$ in events with an amplitude less than the GCR modulation, then at $\gamma = 1.7$ we obtain $J_{10} = J_{100}E_{100}^{\gamma}/E_{10}^{\gamma} = 2.0\left(\text{sm}^2\,\text{s}\,\text{sr}\right)^{-1}$ (below the SPE threshold) and at $\gamma = 3.4$ we obtain $J_{10} = 100$ (cm$^2$ s sr)$^{-1}$ (above the SPE threshold).

Figure 3a plots the ACS SPI light curves for events that exceed the amplitude of GCR modulation (Fig. 1a)—(*1*) October 28, 2021, and (*4*) February 25 and (*7*) July 17, 2023, and during and after the X2.2 flare of February 17, 2023, event 2. In all four of these events in Fig. 3a, after 0 min, increases in the ACS SPI count rate associated with solar HXR radiation are visible. In events 1, 4, and 7, a proton increase in the ACS SPI count rate was observed later than 20 min. We believe that flare 2 could be the source of a similarly powerful SPE given a favorable location on the solar disk. Indeed, according to the data of *SOHO*/EPHIN (Fig. 4), on February 16–17, 2023, a weak proton increase characteristic of eastern events began. It may be associated with a weak flare and fast

**Table 2.** Estimation of proton flux >100 MeV from ACS SPI count rate in selected SPE events

| Options | Events | | | | | |
|---|---|---|---|---|---|---|
| | 1 | 3 | 4 | 6a | 6b | 7 |
| $N_{background}$ | 6843 | 4343 | 4470 | 4242 | 4242 | 4154 |
| $N_{max}$ | 35000 | 5270 | 25000 | 4900 | 4450 | 20500 |
| $J_{100}$ | 0.4 | 0.02 | 0.3 | 0.01 | 0.003 | 0.2 |

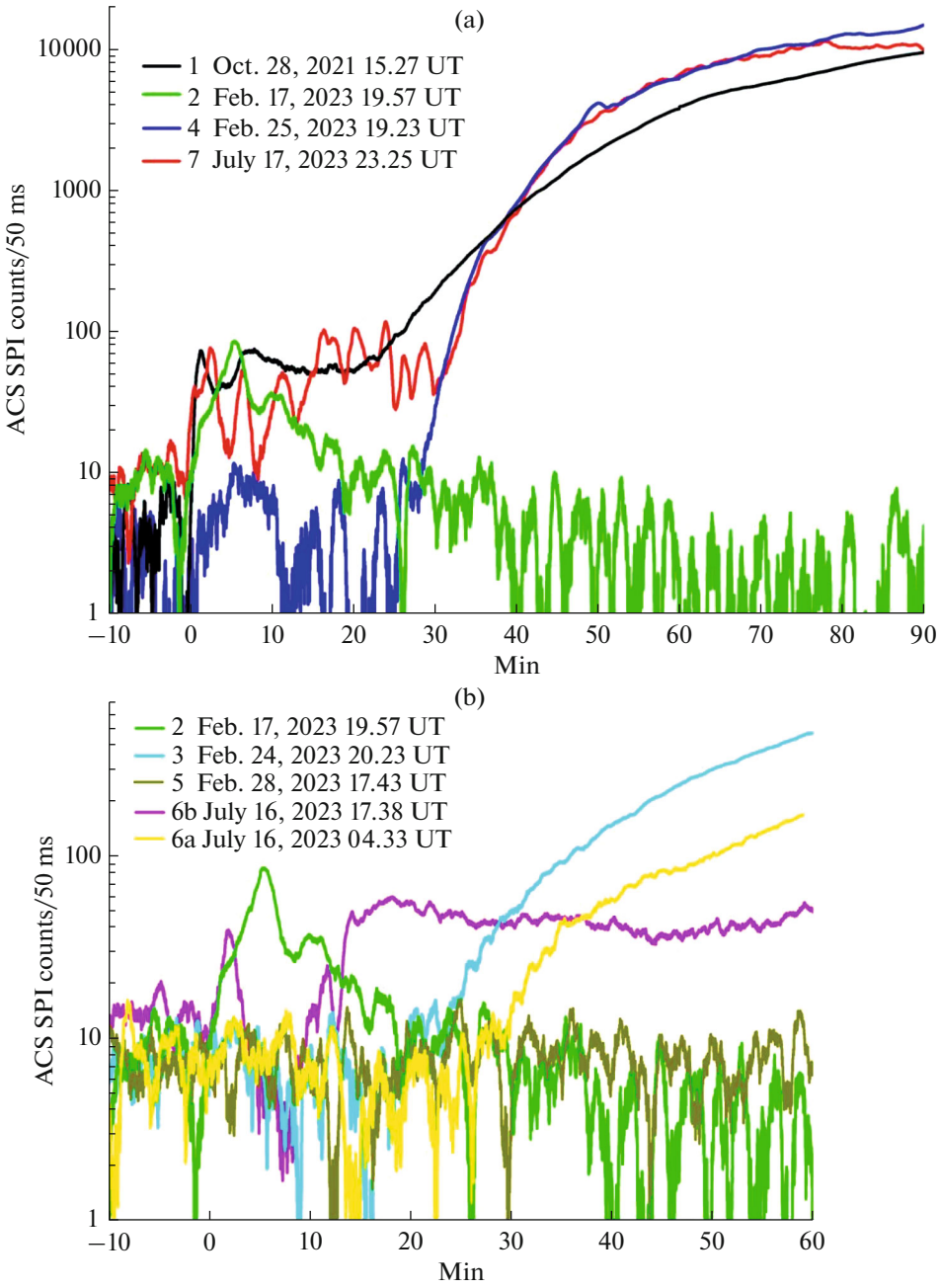


**Fig. 3.** (a) Contribution of solar HXR and protons to the ACS SPI count rate during solar flares and proton events: event 1—X1.1, October 28, 2021; event 2—X2.2, February 17, 2023; event 4—M6.3, February 25, 2023; and event 7—M5.7, August 17–18, 2023. (b) Contribution of solar HXR and protons to the ACS SPI count rate during solar flares and proton events: event 2—X2.2, February 17, 2023; event 3—M3.7, February 24, 2023; event 5—M8.6, February 28, 2023; and event 6a—C1.3 and event 6b—M4.0, July 16, 2023.

CME (10.48 UT, 1549 km/s, PA 301) on February 16 and flare 2 with the CME (20.12 UT, 1315 km/s, PA 56) on February 17.

Solar HXR emission in flares 1, 2, and 7 had comparable maximum intensities, which indicates the interaction of accelerated electrons with a similar spectrum under the same target conditions. The increase in HXR (flare 4) is comparable in amplitude to the ACS SPI background variations, but stands out for its duration and correlation with solar radio emission at 2695 MHz. In case 4, the electron spectrum appeared to be softer and the target less dense. The difference in the temporal structure of the light curves is also noteworthy: in events 1 and 2, there are two maxima, and in case 7 there are eight maxima (Fig. 3a).

The proton increases of events 1, 4, and 7 differed in the time of the first arrival of protons and the rate of increase in the intensity of the ACS SPI count rate.

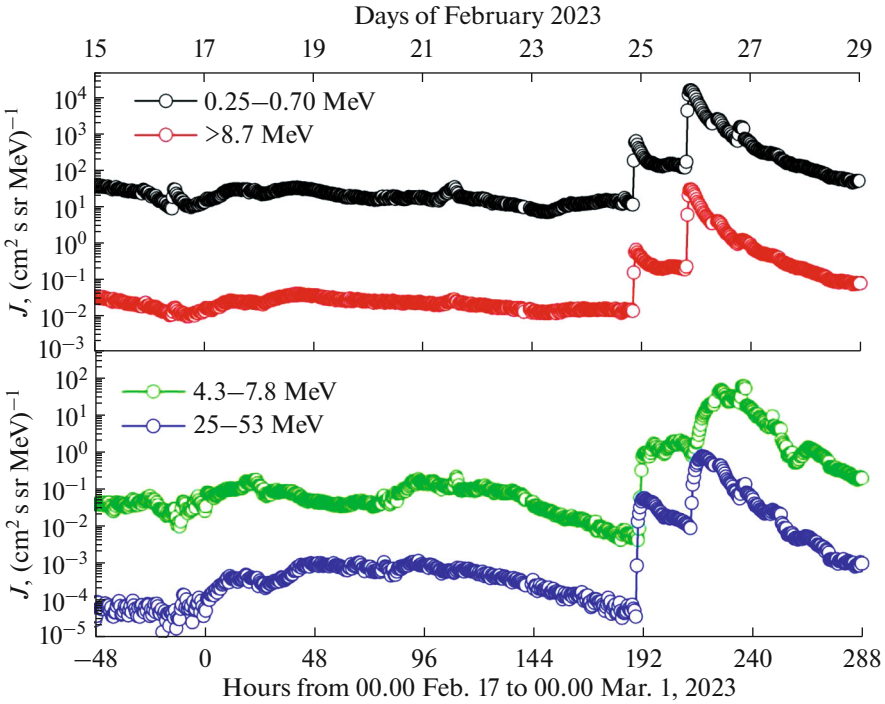


**Fig. 4.** Fluxes of protons and electrons recorded by *SOHO*/EPHIN February 15–28, 2023.

According to the classification of arrival time [6], these events are classified as "late" and "slow." It is reasonable to attribute the difference in the first arrival time estimate of 5 min in events 4 and 7 to the influence of the HXR background with almost identical light curves after 30 min. On the other hand, the rates of proton acceleration in cases 4 and 7 could also differ. The proton increase (flare 4) began at 25 min, and in event 7 it began at 30 min. The arrival delay time of 100-MeV protons at a propagation length of 1.3 AU was ~17 min. The protons had to enter interplanetary space no later than at +8 min in event 4 or +13 min in event 7. The duration of proton acceleration to 100 MeV was ~480 s (flare 4) and ~780 s (flare 7), and the minimum rate of proton acceleration was 100 MeV/480 s = 0.2 MeV/s and 100 MeV/780 s = 0.1 MeV/s.

The difference in the light curve in event 1 from events 4 and 7 to 30 min is most likely due to the high rate of particle acceleration, which is characteristic of GLE events [6]. The minimum proton acceleration rate in the event 1 is 100 MeV/180 s = 0.56 MeV/s. It is possible that the lower rate of acceleration in events 4 and 7 is due to large delays between acceleration episodes that do not overlap (eight HXR maxima in case 7). Since the release of protons into interplanetary space in event 1 was hindered due to the direction of CME propagation (PA value), after approximately 40 min the curve of event 1 is lower than the curves of events 4 and 7. Only outside the time scale (Fig. 3a) will the curve in event 1 be higher than in cases 4 and 7; it was at this time that GLE was observed on neutron monitors [1, 2].

In events 1, 4, and 7, the difference, at least by an order of magnitude, in the maximum intensities of proton fluxes >10 MeV is noteworthy. According to the findings of [21], the GLE event on October 28, 2021 (flare 1), was distinguished by an anomalously hard spectrum. Since the count rates of ACS SPI (protons >100 MeV) and ART-XC in these events were comparable, it can be concluded that protons <100 MeV created virtually no secondary HXR in these detectors and were not a source of additional ionization.

Figure 3b shows the proton increases of curves *3*, *6a*, and *6b*, which are lost in the scale of Fig. 1a, as well as the ACS SPI count rate in events 2 and 5 without proton enhancements. Note that event 5 was observed against the background of a weak increase in the ACS SPI background. Curve *5* in Fig. 3b was obtained after subtracting the straight line $Y = 9.0172 + 0.41853X$, where $X$ is time in minutes relative to zero. A comparison of curves *2* and *5* shows that, in event 5, there was indeed no HXR increase before 20 min, and after 20 min there was no proton increase. In event 3 and 6a there was no HXR increase before 25 min that would correspond to the observed microwave emission. After 25 min in event 3 and 30 min in event 6a, the proton increase began. The required proton acceleration rate in event 3 was 100 MeV/480 s = 0.2 MeV/s. It is not possible to estimate the proton acceleration rate in case 6a due to the uncertainty of the propagation time in the corona and the IS.

In event 6b, there was both an HXR increase and a proton increase in ACS SPI (Fig. 3b), and their characteristics deserve detailed study. Proton acceleration (plasma heating to 12 MK) was delayed by 2 min relative to >100 keV electron acceleration (HXR ACS SPI and 15.4-GHz microwaves). Proton enhancement (6b) was early (first arrival of protons <13 min) and weak (less than 100 ACS SPI counts in 50 ms). The increase by 13 min in case 6b could only be caused by protons >500 MeV, since, if protons began to accelerate by 2 min ($T$ > 20 MK), then they had only 11 min to accelerate and spread. With a propagation length of 1.3 AU, the arrival delay of 500-MeV protons is ~6 min, and the duration of proton acceleration in case 6b will be 5 min. The proton acceleration rate had to be at least >500 MeV/300 s = 1.7 MeV/s. The observation of such an early and weak proton increase suggests that the ACS SPI count rate in event 1 after 10 min may have had a significant contribution from protons >500 MeV.

Thus, in events 1 and 6b, an "early" proton increase in ACS SPI was realized, the proton acceleration rate was ~2 MeV/s (acceleration of electrons to 100 keV in tens of milliseconds is "fast"), and in flares 3, 4 and 7, there was a "late" proton increase, with a proton acceleration rate <0.2 MeV/s (electron acceleration up to 100 keV in hundreds of milliseconds is "slow").

## RADIO EMISSIONS OF THE M6.3 AND M8.6 FLARES ON FEBRUARY 25 AND 8, 2023

This section examines the radio light curves of the RSTN (https://www.ngdc.noaa.gov/stp/space-weather/solar-data/solar-features/solar-radio/rstn-1-second/) in cases 4 and 5, which stand out against the background of other events from Table 1.

Radio emission characteristics for the M6.3 flare on February 25, 2023, presented in Table 1 were taken from the file 20230225events.txt and assigned to the selected zero time. This event stands out because there is no emission information at the extreme frequencies of 245 MHz and 15.4 GHz in the event file for that day. Figure 5a shows the light curves for according to the RSTN (Palehua station, 25feb23.phf) at frequencies with predominant gyrosynchrotron radiation (the highly noisy curve at 15.4 GHz was not plotted). All the curves in Fig. 5a show the beginning of growth no later than zero time (19.23 UT)—the beginning of radiation at 2695 and 1415 MHz, noted in the file (20230225events.txt). However, the beginning of radio emission at a frequency of 8.8 GHz is indicated there at 19.28 UT (5 min); why such a delay was noted is not clear.

The M6.3 flare began significantly earlier than zero time, at 18.40 UT (–43 min). Its trigger was apparently the acceleration of electrons high in the corona, which showed up in the Type VI radio study (a series of Type III bursts lasting more than 10 min). It was observed from 18.37 UT (–46 min) to 20.39 UT (76 min). The light curve at 245 MHz (Fig. 5b) also indicates the development of a flare to zero time in the corona with a plasma concentration of less than $7.4 \times 10^8$ cm$^{-3}$. The light curves at 410, 610, and 1415 MHz (Fig. 5b) show an increase to time zero and indicate changing conditions in the corona (increasing density due to "chromospheric evaporation"). After time zero, the flare developed in the widest possible range of densities, taking into account plasma frequencies (Fig. 5b) and type II radio emission. The onset of the type II burst at 0 min and the appearance of the CME ( 1 min) in the LASCO field of view correspond to the acceleration of the CME before the onset of >100-keV electron acceleration.

Radio emission characteristics for the M8.6 flare on February 28, 2023, presented in Table 1 were taken from the file 20230228events.txt and assigned to the selected zero time. Radio light curves based on RSTN data (Palehua station, 28feb23.phf) are plotted for gyrosynchrotron frequencies in Fig. 6a, and for transition and plasma frequencies in Fig. 6b. As has already been observed in many other events of the 23rd [7] and 24th solar cycles [8, 9], in the M8.6 flare of February 28, 2023, without a CME and SPE, there was no radio emission at frequencies below 1415 MHz. The minimum frequency of radio emissions recorded by RSTN and noted in the file 20230228events.txt was 2695 MHz.

On the panel, Fig. 6a shows two episodes of plasma heating, which correspond to two episodes of radio emission. In the first episode, there is radio emission at the extreme frequencies of 15.4 GHz (Fig. 6a) and 1415 MHz (Fig. 6b), which were not observed in the second episode. The electron spectrum should have been harder, the magnetic field stronger, and the plasma density lower ($2.6 \times 10^{10}$ cm$^{-3}$) than in the second episode ($9.0 \times 10^{10}$ cm$^{-3}$). Thus, the flare was limited in height and did not develop upward into the corona. Bursts of radio emission at 245 MHz, which can be seen in Fig. 6b, were generated independently of processes in the lower atmosphere of the Sun (since there were no bursts at frequencies of 410 and 610 MHz).

## DISCUSSION OF CRITERIA FOR FORECAST OF "PROTON" FLARES

According to the ideas presented in article [22], solar flares occur 0.5–2 days after the detection of a magnetic flux >$10^{13}$ Wb at its ascent speed >$10^9$ Wb/s. However, the onset time of the flares, as well as the specific characteristics of their electromagnetic radiation and particle acceleration, and the appearance of the CME cannot be predicted with greater accuracy. Further, based on the observed characteristics of the solar flare and CME, one can estimate the probability of solar protons entering the heliosphere. A fairly comprehensive overview of the current state of the art of SPE predictive models for 2017 can be found in article [23].

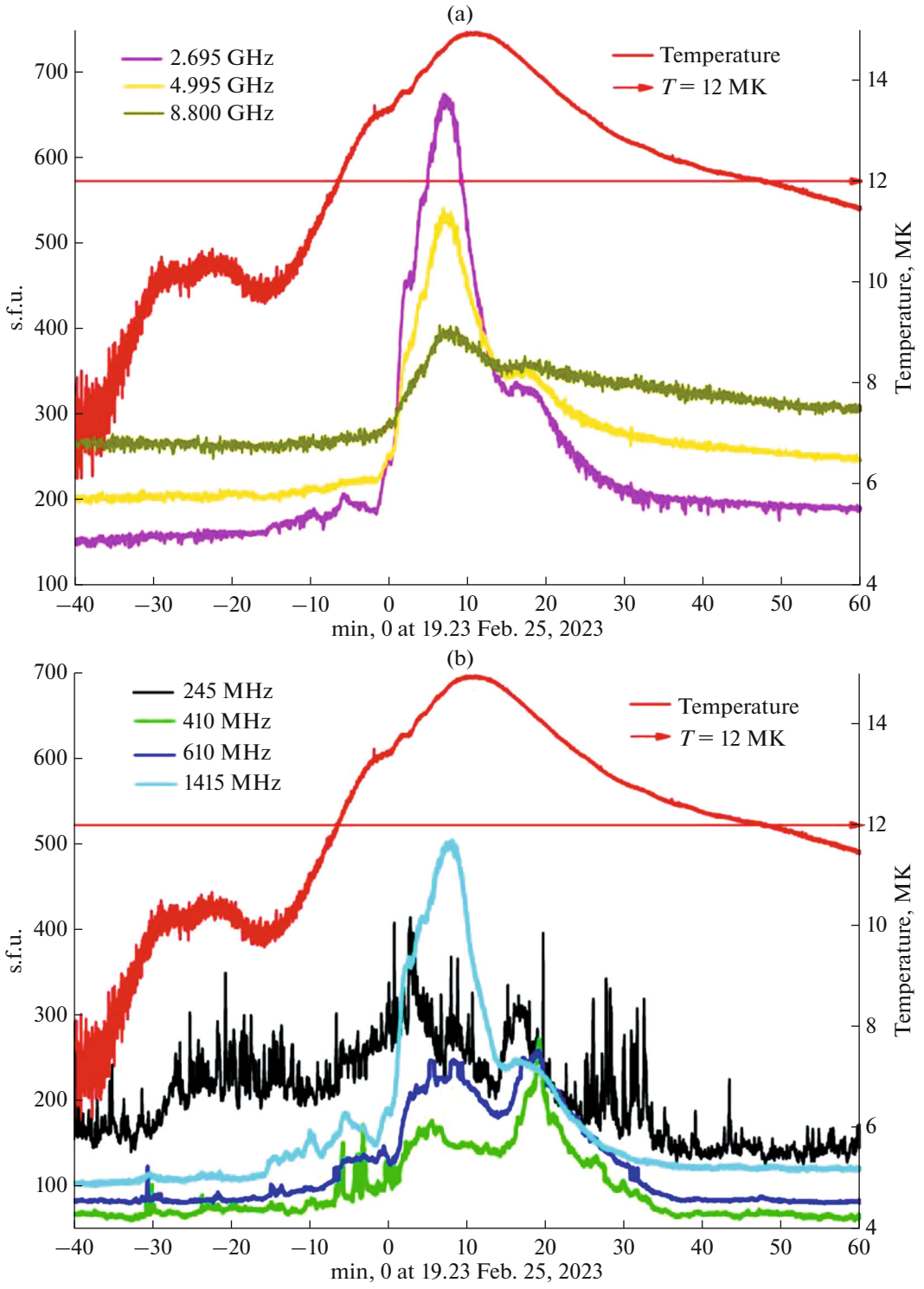


**Fig. 5.** Flare 4 (M6.3) of February 25, 2023. (a) Flare plasma temperature and radio emission flux 8.8 GHz–2695 MHz. (b) Flare plasma temperature and radio emission flux 1415–245 MHz.

Patrol observations of *GOES* based on SXR radiation are available to the consumer in almost real time, so they are widely used for short-term SPE forecasting and testing various statistical prediction models [24–32]. The observational criteria for predicting "proton" flares proposed in [14] generalize and complement the existing methods for predicting SPE from electron and plasma radiation using the

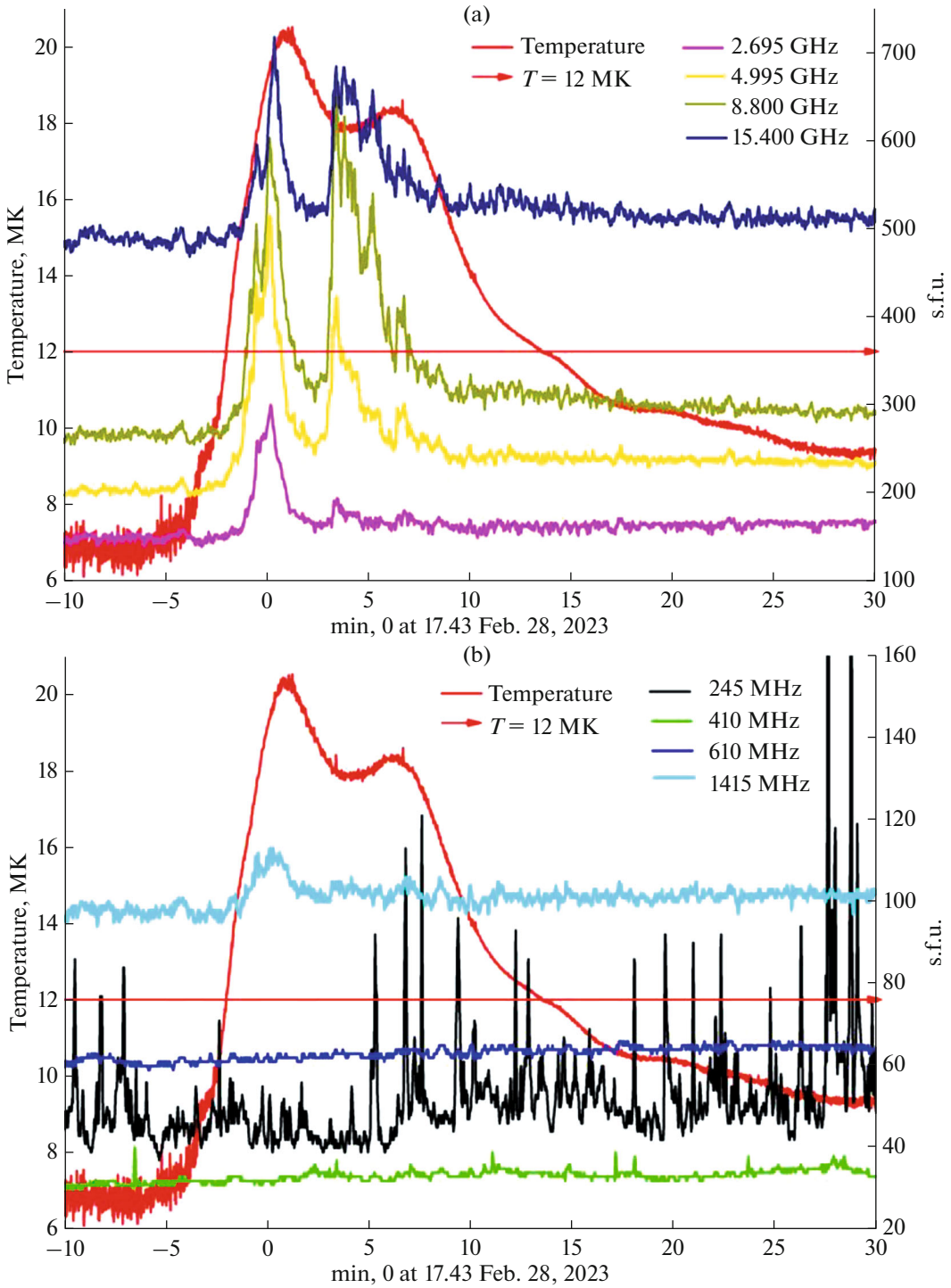


**Fig. 6.** Flare 5 (M8.6) of February 28, 2023. (a) Flare plasma temperature and radio emission flux 15.4 GHz–2695 MHz. (b) Flare plasma temperature and radio emission flux 1415–245 MHz.

parameters of SXR [24–27], HXR [33, 34], microwave [35], and plasma [7] radiation, as well as radio bursts [18].

The authors of [36] drew attention to the observational fact that the impulsive phase of flares with HXR radiation is preceded by a hot SXR onset (a hot X-ray "onset") with a plasma temperature of 10–15 MK. According to estimates in [37], effective additional acceleration of electrons is possible only in the case of a relatively rarefied ($n \lesssim 10^{10}$ cm$^{-3}$) and hot ($T \sim 10^7$ K) background plasma. In the seven cases considered, with the exception of SXR flare events 6a, they began earlier than the selected zero time (row B, Table 1).

Condition for accelerating protons (heating plasma to $T > 12$ MK for more than 5 min according to the *GOES* data) was fulfilled for all selected events except event 6a (line D, Table 1). In six out of eight cases, the flare plasma warmed up to a temperature of >12 MK no later than the zero minute, with the exception of flare 6b, in which this happened at +2 min. In this work, the plasma temperature was not estimated from STIX observations in case 6a, but temperatures usually exceed 12 MK in *X*-flares.

Evidence for long-term electron acceleration >100 keV is given in Table 1: row E is HXR radiation, and row F is microwave radiation. Since the generation of HXR and microwaves depends on the properties of the plasma in which the radiation occurs, comparison of radiation intensities without a detailed analysis of the interaction medium is meaningless. The very fact of recording one of the types of such radiation (microwaves, >2 GHz, or HXR, >100 keV) lasting at least several minutes is important, since at the time of the radiation there may not have been an X-ray or radio receiver capable of measuring it. From this point of view, electron accelerations >100 keV were present in all eight events studied when STIX observations in event 6a are taken into account.

Low-intensity radio bursts are not considered significant in standard SPE prediction techniques (see [35] and references therein). The shortest duration of electron acceleration >100 keV was in event 5, since there was no HXR according to ACS SPI data, and the microwave emission at 15.4 GHz lasted 5 min. The fact that flare 5 would be without a CME and SPE could be confirmed already at 5 min. Radio emission at frequencies <2695 MHz never appeared, suggesting a spatially confined flare. The development of the flare process into the corona (decrease in density, i.e., plasma frequency) is evidenced by plasma radiation (Table 1): row D is the minimum recorded RSTN frequency, row H is the types of recorded continuous radio bursts at frequencies <180 MHz, and row I is the presence of a type II radio burst at frequencies <180 MHz.

Table 1 data show that flares accompanied by SPE are united by the presence of continuous radio bursts at frequencies <180 MHz (column 3 in Table 1). Let us assume that continuous radio emission at frequencies <610 MHz (including radio bursts of II, IV, V, and CTM types) with a duration of more than 5 min is the main evidence of the acceleration of protons on the Sun.

At the beginning of powerful solar flares, when the acceleration of protons has already occurred, but the CME and shock wave have not yet formed, we can expect the release of weak proton fluxes into interplanetary space, as was observed in case 6b. There was no Type II radio emission in events 2, 6a, and 7, despite the presence of a CME with an average velocity of >600 km/s. The speed and direction of propagation of a CME can only be determined after recording its two positions in the field of view of the coronagraph. The duty cycle of CME observations with the LASCO C2 coronagraph is 12 min, so it is impossible to use the CME parameters (row J in Table 1) to predict the moment of the first arrival of solar protons >100 MeV in real time. These parameters are important for assessing the conditions for the release and propagation of protons from the corona into the MP, which determine the time of reaching and the magnitude of the maximum intensity. Also, the ongoing acceleration of the CME in the LASCO field of view indicates the release of energy and acceleration of particles during the posteruptive phase of the flare, which can make a significant contribution to the formation of the temporal profile of the solar proton flux [38].

## CONCLUSIONS

• We analyzed five proton events and HXR increases in the ASC SPI count rate of their parent flares—X1.0 on October 28, 2021; M3.7 on February 24, 2023; and M6.3 on February 25, 2023, as well as M4.0 on July 16, 2023, and M5.7 July 17, 2023. Based on the time of the beginning of the proton increase in ASC SPI, an estimate was made of the duration of proton acceleration and the rate of energy gain by protons.

• In the X1.0 and M4.0 flares, "fast" electron acceleration of ~10 MeV/s was realized ("early" proton increase in ACS SPI, proton acceleration rate ~2 MeV/s), and in the M3.7, M6.3, and M5.7 flares, "slow" electron acceleration ~1 MeV/s was realized ("late" proton increase, proton acceleration rate <0.2 MeV/s).

• Flares accompanied by SPEs are distinguished from the entire population of solar flares by exceeding plasma temperature thresholds (>12 MK), by energy of accelerated electrons (>100 keV), and according to the height of development of flare processes.

• The weak proton boost on the morning of July 16, 2023, could not be predicted by the proposed criteria, since it was the result of an X9 flare on the far side of the Sun detected by STIX on board the *Solar Orbiter*. This outbreak as observed by *GOES* corresponded to score C1.9 and was accompanied by radio emission at a frequency of 245 MHz, long-term continuous radio emission of VI and CTM types at frequencies of 25–180 MHz, and CME acceleration to 1970 km/s.

• The flare of X2.2 (N25E64) on February 17, 2023, satisfied all three criteria for "protonity" and could have become the source of a powerful SPE near the Earth, given a favorable location on the Sun. In the M8.6 (N27W29) flare on February 28, 2023, the third criterion was not met (in terms of the height of development of the flare process), and it, as expected, did not lead to an SPE (developed in plasma with a density $>2.5 \times 10^{10}$ cm$^{-3}$ and plasma frequency >1415 MHz).

• Thus, the considered cycle 25 events show that to predict SPEs with proton energies >100 MeV associated with solar flares, it is necessary to observe the fol-

lowing in real time: SXR radiation in two energy channels, microwave (>3 GHz) and/or HXR radiation, plasma radio emission at frequencies <1415 MHz, and continuous radio bursts of types IV, V, and VI.

## ACKNOWLEDGMENTS

The authors are grateful to the organizers of the First Panasyuk Conference "Problems of Cosmophysics" on July 10–13 in Dubna for the opportunities and hospitality that were provided (the part of the article devoted to the events of February 2023 is based on the materials of the report at this conference) and to A.A. Lutovinov for demonstrating data from the ART-XC radiation monitor and the February 2023 events (ABS and AMS), as well as the participants in space experiments who created the ART-XC, *GOES*, ACS SPI, *SOHO*/EPHIN, *SOHO*/LASCO, and *Solar Orbiter*/STIX databases.

## FUNDING

The work was supported by grants on the topics "Plasma" (ABS and AMS) at the Space Research Institute of the Russian Academy of Sciences and "MAS" (IYUG) at the Main (Pulkovo) Astronomical Observatory of the Russian Academy of Sciences.

## CONFLICT OF INTEREST

The authors of this work declare that they have no conflicts of interest.

## REFERENCES

1. Papaioannou, A., Kouloumvakos, A., Mishev, A., et al., The first ground-level enhancement of solar cycle 25 on 28 October 2021, *Astron. Astrophys.,* 2022, vol. 660, p. L5. https://doi.org/10.1051/0004-6361/202142855
2. Mishev, A.L., Kocharov, L.G., Koldobskiy, S.A., et al., High resolution spectral and anisotropy characteristics of solar protons during the GLE № 73 on 28 October 2021 derived with neutron monitor analyses, *Sol. Phys.,* 2022, vol. 298, no. 7, p. 88. https://doi.org/10.1007/s11207-022-02026-0
3. Klein, K.-L., Musset, S., Vilmer, N., et al., The relativistic solar particle event on 28 October 2021: Evidence of particle acceleration within and escape from the solar corona, *Astron. Astrophys.,* 2022, vol. 663, p. A173. https://doi.org/10.1051/0004-6361/202243903
4. Bazilevskaya, G.A., Cliver, E.W., Kovaltsov, G.A., et al., Solar cycle in the heliosphere and cosmic rays, *Space Sci. Rev.,* 2014, vol. 186, pp. 409–435. https://doi.org/10.1007/s11214-014-0084-0
5. Struminsky, A.B., Grigorieva, I.Yu., Logachev, Yu.I., and Sadovskii, A.M., Solar relativistic electrons and protons on October 28, 2021 (GLE73), *Bull. Russ. Acad. Sci.: Phys.,* 2023, vol. 87, no. 7, pp. 953–957. https://doi.org/10.3103/S1062873823702611
6. Grigorieva, I.Yu., Struminsky, A.B., Logachev, Yu.I., and Sadovskii, A.M., Coronal propagation of solar protons during and after their stochastic acceleration, *Cosmic Res.,* 2023, vol. 61, no. 3, pp. 232–242. https://doi.org/10.1134/S0010952523700235
7. Klein, K.-L., Trottet, G., and Klassen, A., Energetic particle acceleration and propagation in strong CME-less flares, *Sol. Phys.,* 2010, vol. 263, p. 185. https://doi.org/10.1007/s11207-010-9540-5
8. Struminsky, A.B., Grigor'eva I.Yu., Logachev, Yu.I., and Sadovski, A.M., Relationship between duration and rate of the CME acceleration, *Geomagn. Aeron. (Engl. Transl.),* 2021, vol. 61, no. 6, pp. 781–791. https://doi.org/10.1134/S0016793221050133
9. Grigor'eva, I.Yu. and Struminsky, A.B., Flares unaccompanied by interplanetary coronal mass ejections and solar proton events, *Geomagn. Aeron. (Engl. Transl.),* 2021, vol. 61, p. 1263 https://doi.org/10.1134/S0016793221080090
10. Struminskii, A.B., Grigor'eva, I.Yu., Logachev, Yu.I., et al., Solar electrons and protons in the events of September 4–10, 2017 and related phenomena, *Plasma Phys. Rep.,* 2020, vol. 46, no. 2, pp. 174–188. https://doi.org/10.1134/S1063780X20020130
11. Miller, J.A., Cargill, P.J., Emslie, A.G., et al., Critical issues for understanding particle acceleration in impulsive solar flares, *J. Geophys. Res.,* 1997, vol. 102, no. A7, pp. 14631–14660. https://doi.org/10.1029/97JA00976
12. Altyntsev, A.T., Meshalkina, N.S., Lysenko, A.L., et al., Rapid variability in the SOL2011-08-04 flare: Implications for electron acceleration, *Astrophys. J.,* 2019, vol. 883, p. 38. https://doi.org/10.3847/1538-4357/ab380
13. Lysenko, A.L., Frederiks, D.D., Fleishman, G.D., et al., X-ray and gamma-ray emission from solar flares, *Phys. Usp.,* 2020, vol. 63, pp. 818–832. https://doi.org/10.3367/UFNe.2019.06.038757
14. Struminskii, A.B., Sadovskii, A.M., and Grigor'eva, I.Yu., Criteria for forecast of proton events by real time solar observations, *Geomagn. Aeron.,* 2024 (in press).
15. Müller-Mellin, R., Kunow, H., Fleißner, V., et al., COSTEP—comprehensive suprathermal and energetic particle analyser, *Sol. Phys.,* 1995, vol. 162, pp. 483–504.
16. Aschwanden, M.J., The localization of particle acceleration sites in solar flares and CMEs, *Space Sci. Rev.,* 2006, vol. 124, pp. 361–372.
17. Struminskii, A.B., Sadovskii, A.M., and Grigor'eva, I.Yu., Expansion of the soft X-ray source and "magnetic detonation" in solar flares, *Astron. Lett.*, 2023, vol. 49, no. 11, pp. 723–735.
18. Nunez, M. and Paul-Pena, D., Predicting >10 MeV SEP events from solar flare and radio burst data, *Universe,* 2020, vol. 6, p. 161. https://doi.org/10.3390/universe6100161
19. Zheleznykov, V.V. and Zaitsev, V.V., The origin of type-V solar radio bursts, *Sov. Astron.,* 1968, vol. 12, p. 14.
20. Gopalswamy, N., Yashiro, G., Michalek, G., et al., The SOHO/LASCO CME catalog, *Earth, Moon and Planets,* 2009, vol. 104, pp. 295–313. https://doi.org/10.1007/s11038-008-9282-7

21. Chertok, I.M., On some features of the solar proton event on 2021 October 28—GLE73, *Mon. Not. R. Astron. Soc.,* 2022, vol. 517, no. 2, pp. 2709–2713. https://doi.org/10.1093/mnras/stac2843
22. Ishkov, V.N., Predicting solar flare phenomena: Solar proton events, *Bull. Russ. Acad. Sci.: Phys.,* 2023, vol. 87, no. 7, pp. 942–944. https://doi.org/10.3103/S1062873823702763
23. Swalwell, B., Dalla, S., and Walsch, R.W., Solar energetic particle forcasting algorithms and associated false alarms, *Sol. Phys.,* 2017, vol. 292, p. 173. https://doi.org/10.10007/s11207-017-1196-y
24. Garcia, H.A., Forecasting methods for occurrence and magnitude of proton storms with solar soft X rays, *Space Weather,* 2004, vol. 2, p. S02002. https://doi.org/10.1029/2003SW000001
25. Belov, A., Kurt, V., Mavromichalaki, H., et al., Peak-size distributions of proton fluxes and associated soft X-ray flares, *Sol. Phys.,* 2007, vol. 246, no. 2, pp. 457–470.
26. Belov, A.V., Flares, ejections, proton events, *Geomagn. Aeron. (Engl. Transl.),* 2017, vol. 57, no. 6, pp. 727–737. https://doi.org/10.1134/S0016793217060020
27. Alberti, L.M., Cliver, E.W., Storini, M., et al., Solar activity from 2006 to 2014 and short-term forecasts of solar proton events using the ESPERTA model, *Astrophys. J.,* 2017, vol. 838, p. 59. https://doi.org/10.3847/1538-4357/aa5cb8
28. Kahler, S.W., White, S.M., and Ling, A.G., Forecasting $E > 50$-MeV proton events with the proton prediction system (PPS), *J. Space Weather Space Clim.,* 2017, vol. 7, p. A27. https://doi.org/10.1051/swsc/2017025
29. Núñez, M., Predicting solar energetic proton events ($E > 10$ MeV), *Space Weather,* 2011, vol. 9, p. S07003. https://doi.org/10.1029/2010SW000640
30. Núñez, M., Real-time prediction of the occurrence and intensity of the first hours of >100 MeV solar energetic proton events, *Space Weather,* 2015, vol. 13, pp. 807–819. https://doi.org/10.1002/2015SW001256
31. Núñez, M., Predicting well-connected sep events from observations of solar soft X-rays and near-relativistic electrons, *J. Space Weather Space Clim.,* 2018, vol. 8, p. A3.
32. Ling, A.G. and Kahler, S.W., Peak temperatures of large X-ray flares and associated CME speeds and widths, *Astrophys. J.,* 2020, vol. 891, p. 54. doi 103847/1538-4357/ab6f6c
33. Kiplinger, A., Comparative studies of hard X-ray spectral evolution in solar flares with high energy proton events observed at Earth, *Astrophys. J.,* 1995, vol. 453, pp. 973–986. https://doi.org/10.1086/176457
34. Kahler, S.W., Solar energetic particle events and the Kiplinger effect, *Astrophys. J.,* 2012, vol. 747, p. 66. https://doi.org/10.1088/0004-637X/747/1/66
35. Chertok, I.M., Diagnostic analysis of the solar proton flares of September, 2017, *Geomagn. Aeron. (Engl. Transl.),* 2018, vol. 58, pp. 457–463.
36. Hudson, H.S., Simoes, P.J.A., Fletcher, L., et al., Hot X-ray onsets of solar flares, *Mon. Not. R. Astron. Soc.,* 2021, vol. 501, p. 1273. https://doi.org/10.1093/mnras/staa3664
37. Tsap, Yu.T. and Melnikov, V.F., Collisional plasma temperature and betatron acceleration of quasi-thermal electrons in solar flares, *Astron. Lett.,* 2023, vol. 49, no. 4, pp. 200–208. https://doi.org/10.1134/S1063773723040059
38. Grigorieva, I.Yu. and Struminsky, A.B., Formation of sources for solar cosmic rays in eruptive flares X6.9 and M5.1 observed August 9, 2011, and May 17, 2012, *Astron. Rep.,* 2022, vol. 66, no. 6, pp. 481–489. https://doi.org/10.1134/S106377292206004X